CHAPTER 6

CONVENTIONAL SINGLE-PHASE TO THREE-PHASE POWER CONVERTERS

6.1 Introduction

In this chapter the approach to convert single-phase power to three-phase power suitable for powering ac loads is discussed. 'Conventional' power converters used for the conversion of single-phase ac voltage into three-phase power is discussed. Two converter topologies for the Conventional Converters are explained with detailed analysis. The control scheme for the two converter topologies to control the dc voltage and to achieve unity power factor operation is also discussed. An induction machine was used as a load for the two converter topologies, which was simulated in Matlab/Simulink to verify the functionality of the converters.

6.2 Single-Phase To Three-Phase Power Conversion

The main function of the Three-phase electrical equipment such as three-phase ac motors are significantly more efficient, economical and easy to control then their single-phase counterpart. The size of the three-phase motors, for the same power rating as that of the single-phase motor is relatively small. Three-phase power is not usually available in many of the rural or light industrial areas, due to the high cost of extending the three-phase service. So the only available power in many instances will be single-phase power and so there exists a need for converters which can convert

single phase power to three phase power keeping in mind the considerations of cost and good performance.

6.2.1.Conventional Single Phase to Three-Phase Power Converter Circuits

In the classical method of single-phase to three-phase conversion the single-phase power supply is given to the converter, which can either be full, or half bridge type, in cascade with a three-phase inverter with a dc link capacitor in between. The general concept of conventional circuits is as shown in Fig 6.1.

In the conventional converters the ac-to-dc conversion is independent from the dc-to-ac conversion. The power supply current is controlled to be sinusoidal by the full-bridge ac-to-dc converter, while the pulse-width modulation inverter controls the motor input voltage. These two control actions are independent and a large capacitor is inserted in between the converters for decoupling.

The work of the single-phase inverter is to generate dc voltage at its output terminals and all that the three-phase inverter requires is dc voltage with little or no ripple at its input terminals. The converter connected to the supply is called the line-side converter and the one connected to the load is the load-side converter. Thus in the conventional topologies the control of the line and the load side converters are independent.

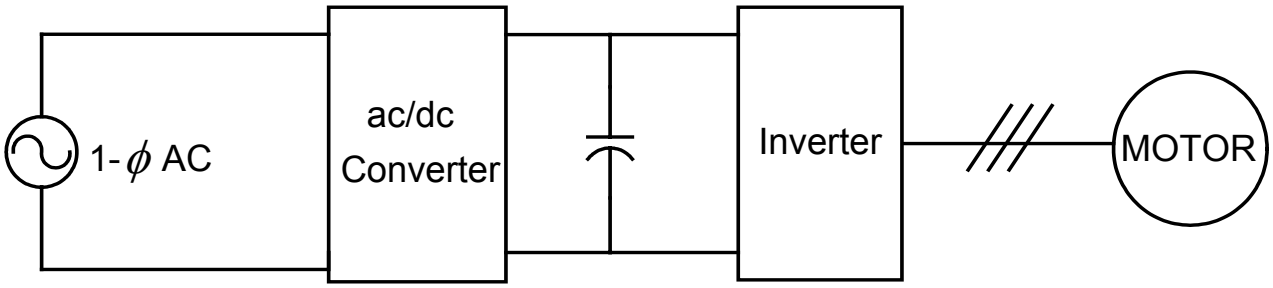

Figure 6.1: Concept of conventional circuits.

Two types of conventional single-phase to three-phase conversion topologies are discussed in the following sections with detailed analysis of the mathematical model.

6.2.1.1. Conventional Full-Bridge Topology

The 'conventional' full bridge converter is capable of bidirectional power transfer, which is power being exchanged between the load and the supply in either way. The full bridge topology as shown in Figure 6.2 has four switches for the ac-to-dc conversion. The dc voltage at the output terminals of this conversion process is fed into a three-phase inverter which produces the three phase balanced voltages across the load. In the topology in Figure 6.2 the power transfer is quite apparent, that is the single phase supply is applied between the two midpoints of the two converter legs and a big capacitor is kept at the output terminals, which also serves as a filter. The dc voltage across the capacitor is applied to the three-phase inverter, which can be in the Voltage Source Inverter (VSI), or the Current Source Inverter (CSI) topology in which the switches can be PWM operated or normal thyristor fired circuit.

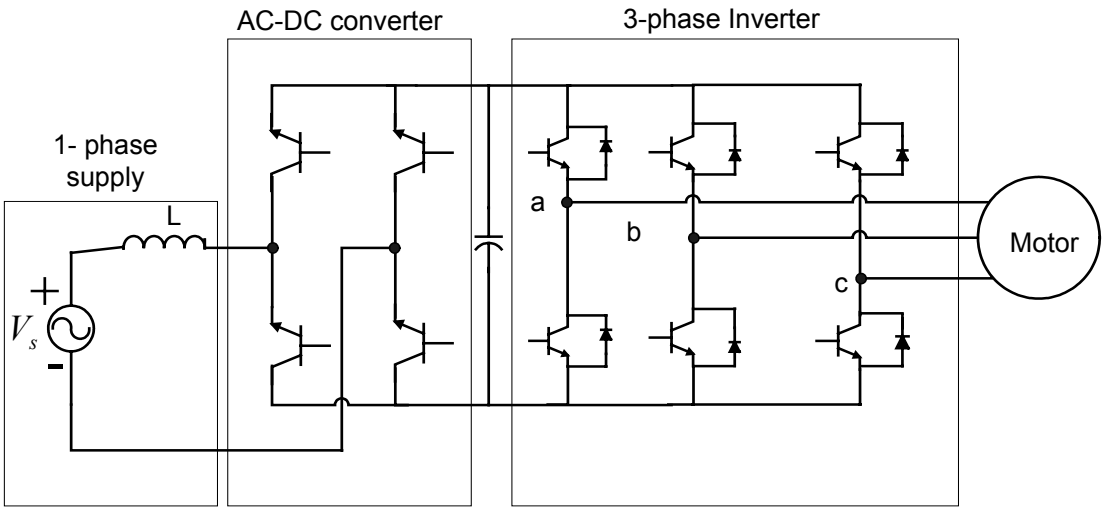

Figure6.2: Conventional full-bridge ac/dc converter inverter circuit.

In the above explained circuit topology there is an input reactor to reduce the ripple in the supply current, which arises due to the fact that the converters have switching devices which would continuously be turned ON and turned OFF according to a predetermined pattern leading to pulsating the input current.

6.2.1.2 Conventional Half-Bridge Topology

The half bridge topology as shown in Figure 6.3 is similar to a full bridge one except that a capacitor leg with neutral accessible replaces one of the converter legs of the line side converter, but the load side converter remains the same. This topology is cheaper when compared to the full bridge type as it involves less number of switches but the size of the converter increases due to the capacitor.

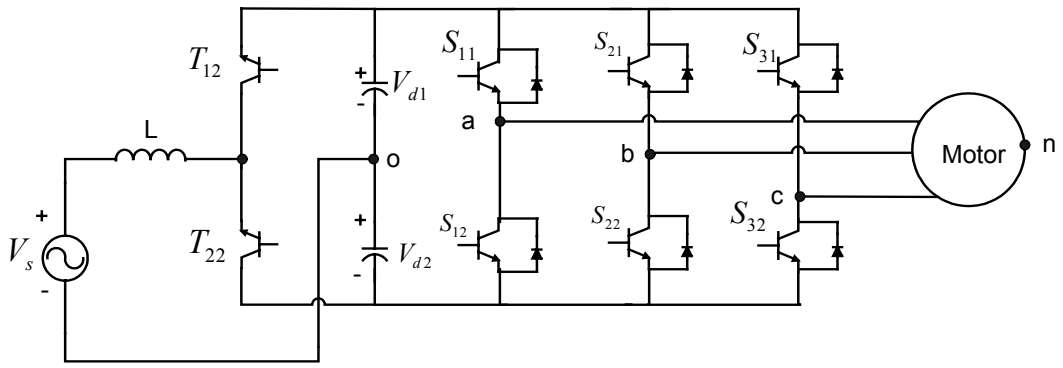

Figure 6.3: Conventional Half-Bridge Circuit.

In the half bridge converter the dc link voltage will be twice that in a full bridge converter, and so the switching devices must withstand this increased voltage. But this topology is useful when the output voltage is not too high, or for low power applications. The equations which describe the operation of the converter in Figure 6.3 based on Kirchoff's voltage law (KVL), are

$$\frac{V_d}{2}(T_{11} - T_{12}) = V_s - L\frac{di_s}{dt} \tag{6.1}$$

$$\frac{V_d}{2}(S_{11} - S_{12}) = V_{an} + V_{no} \tag{6.2}$$

$$\frac{V_d}{2}(S_{21} - S_{22}) = V_{bn} + V_{no} \tag{6.3}$$

$$\frac{V_d}{2}(S_{31} - S_{32}) = V_{cn} + V_{no}\,. \tag{6.4}$$

where V_{no} is the voltage between the neutral point of the load and the midpoint of the dc-link voltage. As the switching functions for the two devices in the same leg are complementary then;

$$T_{11} + T_{12} = 1 \tag{6.5}$$

$$S_{11} + S_{12} = 1 \tag{6.6}$$

$$S_{21} + S_{22} = 1 \tag{6.7}$$

$$S_{31} + S_{32} = 1 \quad . \tag{6.8}$$

Adding the Equations in 6.2 to 6.4 together, Equation 6.9 is obtained

$$\frac{V_{DC}}{2}(S_{11} + S_{21} + S_{31} - S_{12} - S_{22} - S_{32}) = V_{an} + V_{bn} + V_{cn} + 3V_{no} \tag{6.9}$$

By considering balanced voltages, $V_{an} + V_{bn} + V_{cn}$ = 0 and making use of the conditions from Equations 4.1 to 4.3, Equation 4.7 becomes

$$\frac{V_{DC}}{6}(2S_{11} + 2S_{21} + 2S_{31} - 3) = V_{no} \tag{6.10}$$

Substituting for V_{no} in Equations 4.4 to 4.6,

$$\frac{V_{DC}}{3}(2S_{11} - S_{21} - S_{31}) = V_{an} \tag{6.11}$$

$$\frac{V_{DC}}{3}(2S_{21} - S_{21} - S_{31}) = V_{bn} \tag{6.12}$$

$$\frac{V_{DC}}{3}(2S_{31} - S_{21} - S_{11}) = V_{cn} \quad . \tag{6.13}$$

Using the conditions in Equations from 6.5 to 6.8 Equations 6.1 - 6.4 become

$$\frac{V_d}{2}(2T_{11} - 1) = V_s - L\frac{di_s}{dt} \tag{6.14}$$

$$\frac{V_d}{2}(2S_{11} - 1) = V_{an} + V_{no} \tag{6.15}$$

$$\frac{V_d}{2}(2S_{21}-1) = V_{bn} + V_{no} \tag{6.16}$$

$$\frac{V_d}{2}(2S_{31}-1) = V_{cn} + V_{no} \quad . \tag{6.17}$$

Replacing the switching functions in the above equations with the modulation signals the above equations are modified as given in Equations 6.18 to 6.21.

$$\frac{V_d}{2}M_{tt} = V_s - L\frac{di_s}{dt} \tag{6.18}$$

$$\frac{V_d}{2}M_{11} = V_{an} + V_{no} \tag{6.19}$$

$$\frac{V_d}{2}M_{21} = V_{an} + V_{no} \tag{6.20}$$

$$\frac{V_d}{2}M_{31} = V_{an} + V_{no} \quad . \tag{6.21}$$

The above equations can be written in the matrix form as,

$$\frac{V_d}{2}\begin{bmatrix} M_{11} \\ M_{21} \\ M_{31} \end{bmatrix} = \begin{bmatrix} V_{an} \\ V_{bn} \\ V_{cn} \end{bmatrix} + \begin{bmatrix} V_{no} \\ V_{no} \\ V_{no} \end{bmatrix}. \tag{6.22}$$

Transforming the above matrix equations in to the synchronous reference frame, constant values for modulation index are obtained which makes the control scheme simple to be implemented, as the control of dc variables or quantities is not as complicated as those with varying quantities.

Thus by transforming the matrix equations in 6.23, Equations in 6.18 are obtained.

$$\frac{V_d}{2}\begin{bmatrix} m_{qs} \\ m_{ds} \\ m_{os} \end{bmatrix} = \begin{bmatrix} V_{qs} \\ V_{ds} \\ 0 \end{bmatrix} + \begin{bmatrix} 0 \\ 0 \\ V_{no}/3 \end{bmatrix} \tag{6.23}$$

Thus,

$$m_{qs} = \frac{2V_{qs}}{V_d} \tag{6.24}$$

$$m_{ds} = \frac{2V_{ds}}{V_d} \tag{6.25}$$

$$m_{os} = \frac{2V_{no}}{3V_d} \ . \tag{6.26}$$

In Equation 6.21 the zero sequence voltage can be assumed to be zero or some value, which leads to discontinuous PWM scheme. In the analysis that follows here V_{no} is assumed to be zero.

The dc –link current equation can be written as the sum of each of the load current and the supply current as,

$$CpV_d = 2(i_s T_{11} - i_a S_{11} - i_b S_{21} - i_c S_{31}) \tag{6.27}$$

or equivalently

$$CpV_d = (i_s T_{11} - \frac{1}{2}(i_a M_{11} - i_b M_{21} - i_c M_{31})) \tag{6.28}$$

Apply the synchronous reference frame transformation to the above equation by making use of the following equalities,

$$i_{qdo}{}^{T} = [(K_s) i_{abc}]^{T} = \; i_{abc}{}^{T} K_s{}^{T} \tag{6.29}$$

$$i_{abc}{}^{T} = i_{qdo}{}^{T} (K_s{}^{T})^{-1} \tag{6.30}$$

Therefore, the dc link current can be written as

$$CpV_d = (i_s T_{11} - \frac{1}{2}(i_{abc}{}^{T} M_{112131})) \tag{6.31}$$

where $i_{abc}{}^{T} = [i_a \; i_b \; i_c]^{T}$ and $M_{112131} = \begin{bmatrix} M_{11} \\ M_{21} \\ M_{31} \end{bmatrix}$

Using 'qdo' transformation for Equation 6.31 the equation for the dc link current becomes,

$$CpV_d = (i_s T_{11} - \frac{1}{2}(i_{qdo}{}^{T} (K_s{}^{T})^{-1} (K_s)^{-1} m_{qdo})) \tag{6.32}$$

where $m_{qdo} = [m_{qs} \; m_{ds} \; m_{os}]$ and $(K_s{}^{T})^{-1}(K_s)^{-1} = \begin{bmatrix} \frac{3}{2} & 0 & 0 \\ 0 & \frac{3}{2} & 0 \\ 0 & 0 & 3 \end{bmatrix}$,

Hence Equation 6.27 becomes ,

$$CpV_d = (i_s T_{11} - 1.5 m_{qs} i_{qs} - 1.5 m_{ds} i_{ds}) \tag{6.33}$$

or

$$i_s T_{11} = CpV_d + 1.5 m_{qs} i_{qs} + 1.5 m_{ds} i_{ds} \quad . \tag{6.34}$$

The zero sequence is assumed to be zero or in other words the three phase currents add up to zero. Equations 6.24 to 6.26 and Equation 6.36 constitute the basic equations for the control of the machine. The control strategy and the principle of control is as explained in the following section.

6.2.2 Controller Design For The Half-Bridge Converter

The control objective for the line side converter is to achieve unity power factor for the supply voltage and the current while maintaining a constant dc bus voltage. The way it is done is as explained, the dc voltage is controlled to be constant at a determined value.

When the load current increases or decreases, it is the single phase supply which should compensate for it, thus as the dc magnitude is controlled to be constant the amount it deviates from the actual value is proportional to the amount of current which the supply has to give out, following any change. Thus the magnitude for the supply current is obtained, this magnitude, is to be in phase with the supply voltage for which a sinusoidal waveform synchronous with the power supply is obtained by measuring the power supply voltage and dividing it by its peak value. This gives the reference for the supply current.

The actual supply current is calculated and compared with the reference and this change is accounted by the line side converter, by changing the modulation index for the switching devices. Changing the modulation means the modulation index of

the switching signals is increased or decreased which affects the amount the switching devices conduct thus affecting the fundamental current component.

6.2.2.1 Stationary Reference Frame controller

The controller structure with a PI would work effectively on for only dc quantities but not when the control variable is a time varying quantity as in the above case where the zero sequence current I_s is not a dc quantity. Hence, the conventional PI controller cannot be used for its control, thus a stationary reference frame controller is employed whose structure is explained in the block diagram form is outlined in Figure 6.4 [23].

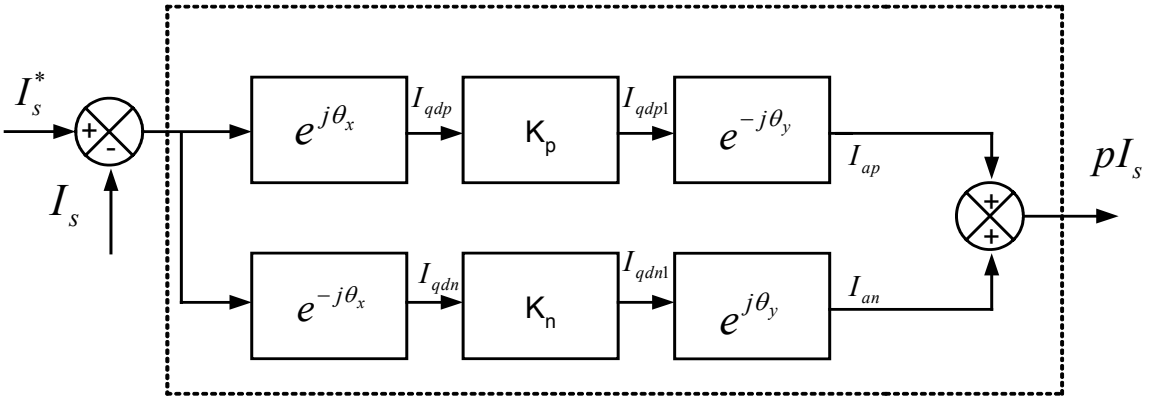

Figure 6.4: Structure of the Stationary Reference Frame Controller

The errors of the currents are firstly converted to positive and negative synchronous reference frames i.e., θ_x and $-\theta_x$. Hence the output of the transformation block is:

$$I_{qdp} = (I_s^* - I_s)e^{i\theta_x} \tag{6.35}$$

$$I_{qdn} = (I_s^* - I_s)e^{-i\theta_x} \tag{6.36}$$

where, $\theta_x = \omega_e t + \theta_{x0}$; θ_{x0} - Initial reference angle

These signals are passed through two controllers whose transfer functions are given by K_p (p) and K_n (p). Hence the output of the regulators is:

$$I_{qdp1} = (I_s^* - I_s)e^{i\theta_x}K_p(p) \tag{6.37}$$

$$I_{qdn} = (I_s^* - I_s)e^{-i\theta_x}K_n(p) \tag{6.38}$$

Now these signals are again transformed back to the abc reference frame with some delay angle ϕ_1 i.e., $\theta_y = \omega_e t + \theta_{x0} - \phi_1, \theta_y = -\omega_e t + \theta_{x0} - \phi_1$. Hence the resulting signals from these transformation blocks are:

$$I_{sp} = (I_s^* - I_s)e^{i(\theta_x - \theta_y)}K_p(p - j\omega) \tag{6.39}$$

$$I_{an} = (I_a^* - I_a)e^{-i(\theta_x - \theta_y)}K_n(p + j\omega) \tag{6.40}$$

Let $\theta_x - \theta_y = \phi_1$, then:

$$I_{sp} = (I_s^* - I_s)e^{i\phi_1}K_p(p - j\omega) \tag{6.41}$$

$$I_{sn} = (I_s^* - I_s)e^{-i\phi_1}K_n(p + j\omega) \tag{6.42}$$

Now summing the two signals I_{sp}, I_{sn} to get the output of the controller, which is assumed to be equal to pI_s.

$$pI_s = (I_s^* - I_s)e^{i\phi_1}K_p(p - j\omega) + (I_s^* - I_s)e^{-i\phi_1}K_n(p + j\omega);$$
$$\Rightarrow (I_s^* - I_s)[e^{i\phi_1}K_p(p - j\omega) + e^{-i\phi_1}K_n(p + j\omega)]$$

By simplifying the above equation the transfer function of the system as:

$$\frac{I_s}{I_s^*} = \frac{e^{i\phi_1}K_p(p - j\omega) + e^{-i\phi_1}K_n(p + j\omega)}{p + e^{i\phi_1}K_p(p - j\omega) + e^{-i\phi_1}K_n(p + j\omega)} \tag{6.43}$$

In this particular case let us assume the controller to be a PI controller whose transfer function is given as

$$K_p(p) = k_p + \frac{k_{ip}}{p}$$
$$K_n(p) = k_n + \frac{k_{in}}{p} \tag{6.44}$$

Hence, by substituting the above transfer functions in (6.43) and simplifying the overall transfer function becomes

$$\frac{I_s}{I_s^*} = \frac{e^{i\phi_1}(p+j\omega)[k_p(p-j\omega)+k_{ip}] + e^{-i\phi_1}(p-j\omega)[k_n(p+j\omega)+k_{in}]}{p(p^2+\omega^2) + e^{i\phi_1}(p+j\omega)[k_p(p-j\omega)+k_{ip}] + e^{-i\phi_1}(p-j\omega)[k_n(p+j\omega)+k_{in}]} \tag{6.45}$$

For simplicity, if $k_{ip} = k_{in} = k_i; k_n = k_p = k_p$, then

$$\frac{I_s}{I_s^*} = \frac{p^2 2k_p \cos\phi_1 + p2k_i \cos\phi_1 + 2\cos\phi_1\omega^2 k_p - \omega\sin\phi_1}{p^3 + p^2 2k_p \cos\phi_1 + p[2k_i \cos\phi_1 + \omega^2] + 2\cos\phi_1\omega^2 k_p - \omega\sin\phi_1} \tag{6.46}$$

In designing the parameters of the controller, the denominator of the transfer function is compared with Butterworth Polynomial. The Butter-worth method locates the eigen values of the transfer function uniformly in the left half of the s-plane, on a circle of radius ω_o , with its center at the origin. The Butterworth polynomials for a transfer function with a third order denominator is given as:

$$p^3 + 2p^2 w_0 + 2pw_0^2 + w_0^3 = 0 \tag{6.47}$$

Hence by comparing the denominator of the transfer function with above polynomial

$$k_p = \frac{w_0}{\cos\phi_1} \quad ; \; k_i = \frac{2w_0^2 - \omega^2}{2\cos\phi_1}; \; w_0 = (2\cos\phi_1\omega^2 k_p - \omega\sin\phi_1)^{1/3}$$

The zeros of the system are found by equating the numerator of the transfer function to zero. Hence

$$p^2 2k_p \cos\phi_1 + p2k_i \cos\phi_1 + 2\cos\phi_1 \omega^2 k_p - \omega \sin\phi_1 = 0 \tag{6.48}$$

By solving the equations the two zeros of the system are obtained as:

$$Z_1, Z_2 = \frac{-2k_i \cos\phi_1 \pm \sqrt{4k_i^2 \cos^2\phi_1 - (8k_p \cos\phi_1)(2\cos\phi_1 \omega^2 k_p - \omega \sin\phi_1)}}{4k_p \cos\phi_1}$$

For zeros to be real the following conditions has to be satisfied:

$$k_i > \left[2\omega k_p \left[2\omega k_p - \tan\phi_1\right]\right]^{1/2}$$

The condition for zeros to lie in the negative half plane, which corresponds to marking the system to be minimum-phase when the roots are real,

$$k_p > \frac{\tan\phi_1}{2\omega}$$

The condition for zeros to be complex numbers is:

$$k_i < \left[2\omega k_p \left[2\omega k_p - \tan\phi_1\right]\right]^{1/2}$$

When the roots are complex numbers, the condition for zeros to lie in the negative half plane, is $\frac{k_i}{k_p} > 0$

Now the transfer function of the controller $G_{AC}(s)$ is to be found. From Fig. 6.4 $G_{AC}(s)$ can be written as

$$G_{AC}(s) = \frac{pI_s}{I_s^* - I_s} \tag{6.49}$$

$$\frac{pI_s}{I_a^* - I_s} = [e^{i\phi_1} K_p (p - j\omega) + e^{-i\phi_1} K_n (p + j\omega)] \tag{6.50}$$

Let

$$K_p(p) = k_p + \frac{k_{ip}}{p}$$

$$K_n(p) = k_n + \frac{k_{in}}{p}$$

Hence by substituting the transfer functions of the PI controllers and assuming $k_{ip} = k_{in} = k_i; k_n = k_p = k_p$ and simplifying the expression for $G_{AC}(s)$ becomes,

$$G_{AC}(s) = \frac{pI_s}{I_s^* - I_s} = \frac{p^2 2k_p \cos\phi_1 + p2k_i \cos\phi_1 + 2k_p \cos\phi_1 \omega^2}{p^2 + \omega^2} \tag{6.51}$$

Hence after obtaining the transfer function of the controller, the k_p and k_i values are obtained as explained above and hence the controller is used to control the current.

6.2.3 Overall Control Block Diagram

Equations 6.25 to 6.26 constitute the basic equations for the controller. The controller design using the feedback linearization is explained in Chapter 5. Equations 6.25 to 6.26 model the load. The load modeling was the key concept of Chapter 5 and so it is not discussed here again. For the line side converter the modulation signal is obtained from Equation 6.18. Equation 6.18 can be written as,

$$M_{tt} = \frac{2}{V_d}(V_s - LpI_s) \tag{6.52}$$

which is the modulation signal for the fourth leg.

In Equation 6.34, the product of the term $i_s T_{11}$ is the product of two time varying signals of the same frequency hence the product gives a fundamental

component and a second harmonic component, so equating terms on either side the second harmonic component gets cancelled and so Equation 6.34 can be written as

$$i_s = CpV_d + 1.5m_{qs}i_{qs} + 1.5m_{ds}i_{ds} \quad (6.34\ b)$$

The overall controller structure is shown in Figure 6.5. Some of the equations in Figure 6.5 correspond to Chapter 5 of this thesis, which are not rewritten here to avoid duplication.

6.2.4.Simualtion Results

The Conventional half-bridge circuit in Figure 6.3 was simulated using an induction machine as load using the control structure as shown in Figure 6.5. The simulation results include some key parameters for the load and also show the actual quantities follow the reference values. The speed reference in this case was ramped up from zero to the rated motor speed of 207.3 rad/sec. The parameters for the machine (load) are given in Appendix A. Figures 6.6 to 6.9 show the simulation results for the discussed converter topology, when initially the motor is running on no-load and at 1s a load of 4N-m is added on the machine and the system is allowed to settle and then the load was removed at 3s.

Figure 6.6(a) shows the dc voltage is regulated to 700 V, it can be seen that the voltage reduces slightly when the load is added but it gradually builds up to be constant at 700 V, 6.6(b) shows the the rotor flux controlled at a constant value is shown as can be seen the actual value follows the command very closely.

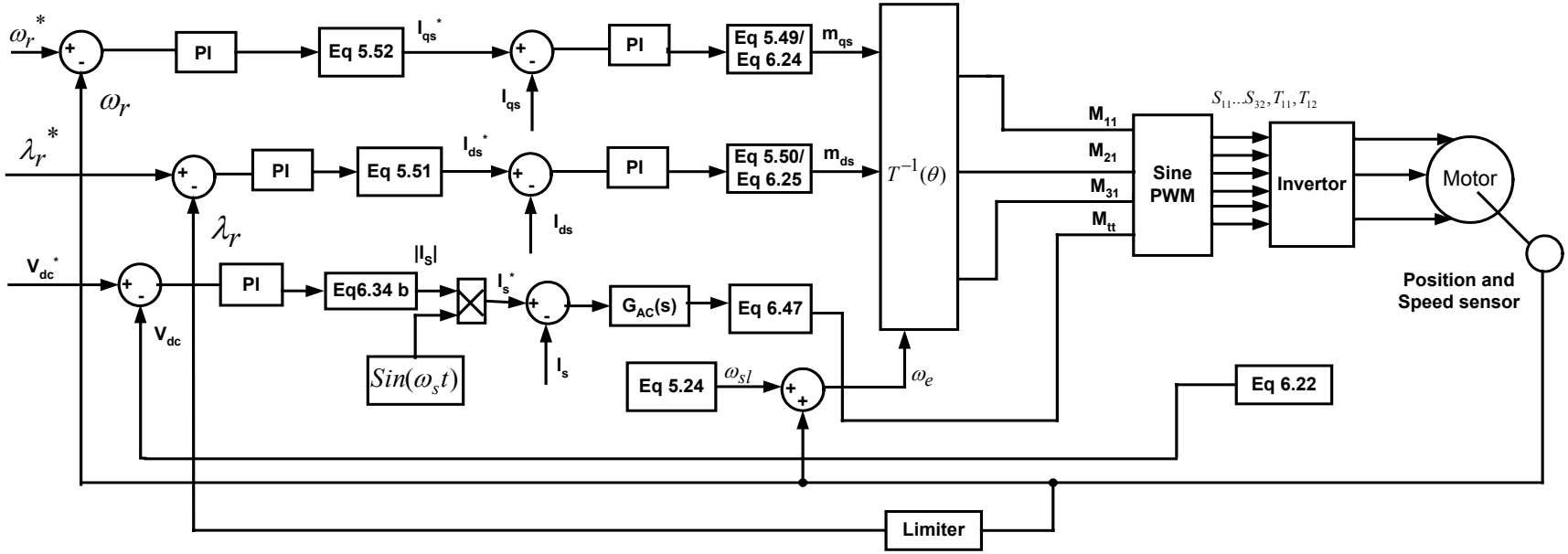

Figure 6.5: Control Block diagram for the Conventional Half-Bridge Converter.

Figure 6.7(a) and 6.7(b) shows the motor frequency and the rotor speed, following any change it can be seen that to keep the rotor speed constant the motor frequency is slightly increased. Figure 6.7 (c) and (d) show the slip speed and the electromagnetic torque when a load torque of 4 N-m is added on to the machine.

In Figure 6.8(a) the three-phase load currents are plotted against time when the load on the machine persists. Figure 6.8(b) shows the supply voltage and current, which are almost in phase with each other. The supply voltage is scaled by some factor so that both the voltage and current can be seen clearly. Figure 6.8 (c) shows the modulation signals for the four switching legs. The modulation signals for the three legs connected to the three-phases are balanced, and the modulation signal for the fourth leg is of the same frequency as the supply. In Figure 6.9(a) the unfiltered phase voltages are plotted against time while in Figure6.9 (b), (c) ,(d) the filtered load voltages are plotted against time .

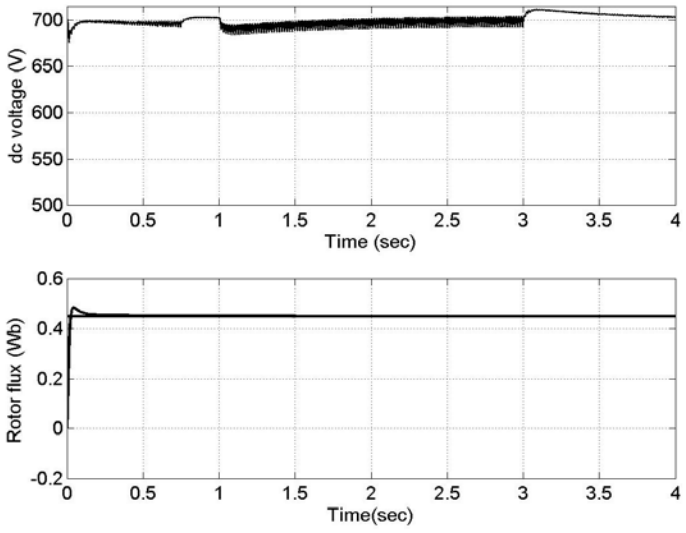

(a)

(b)

Figure 6.6: Regulated dc voltage (a) The dc link voltage for a load change of 4 N-m, (b) the rotor flux linkages.

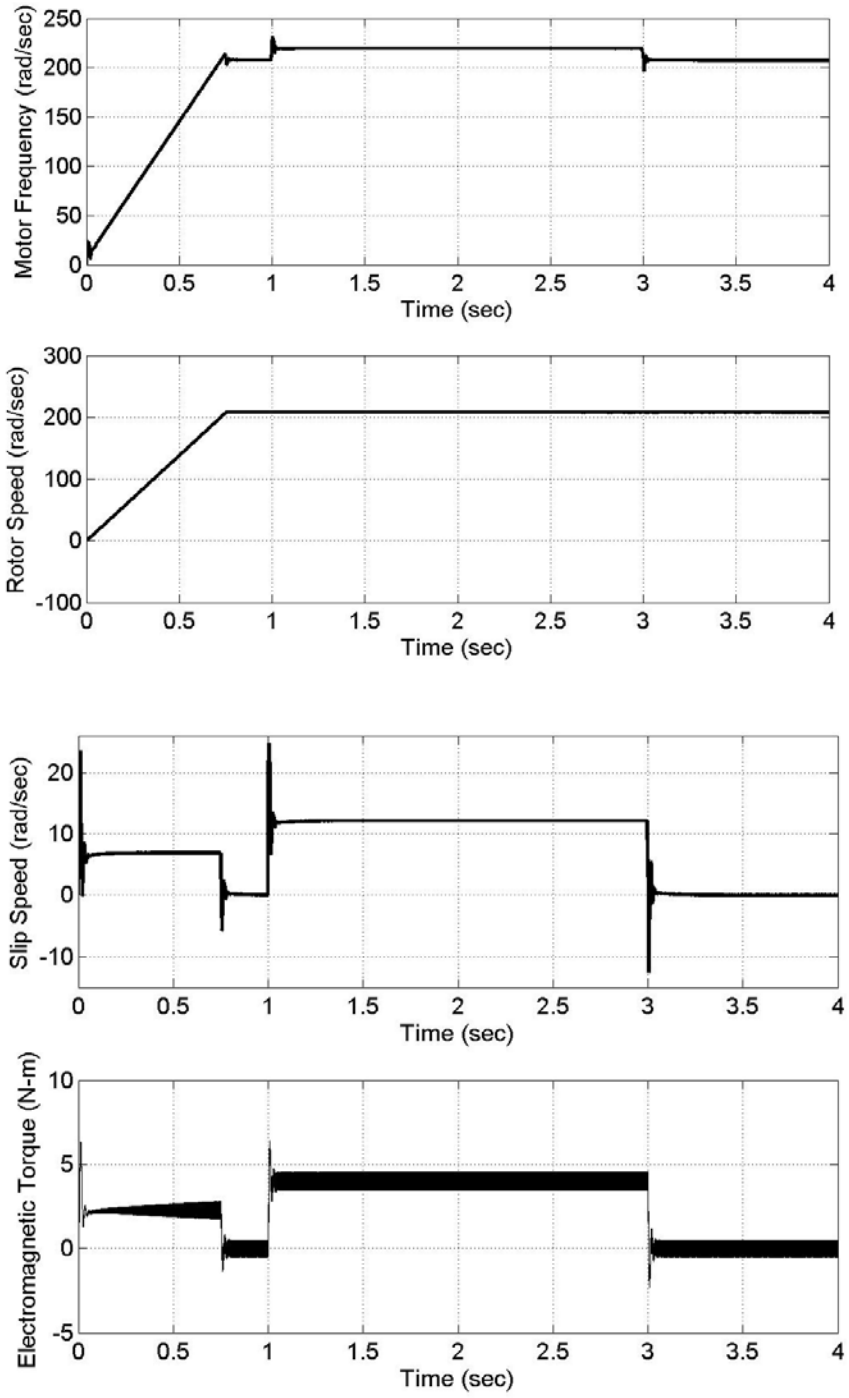

Figure 6.7: Load change. (a) The motor frequency in rad/sec, (b) The rotor speed and the command in rad/sec, (c) the slip speed, (d) the electromagnetic torque of 4N-m.

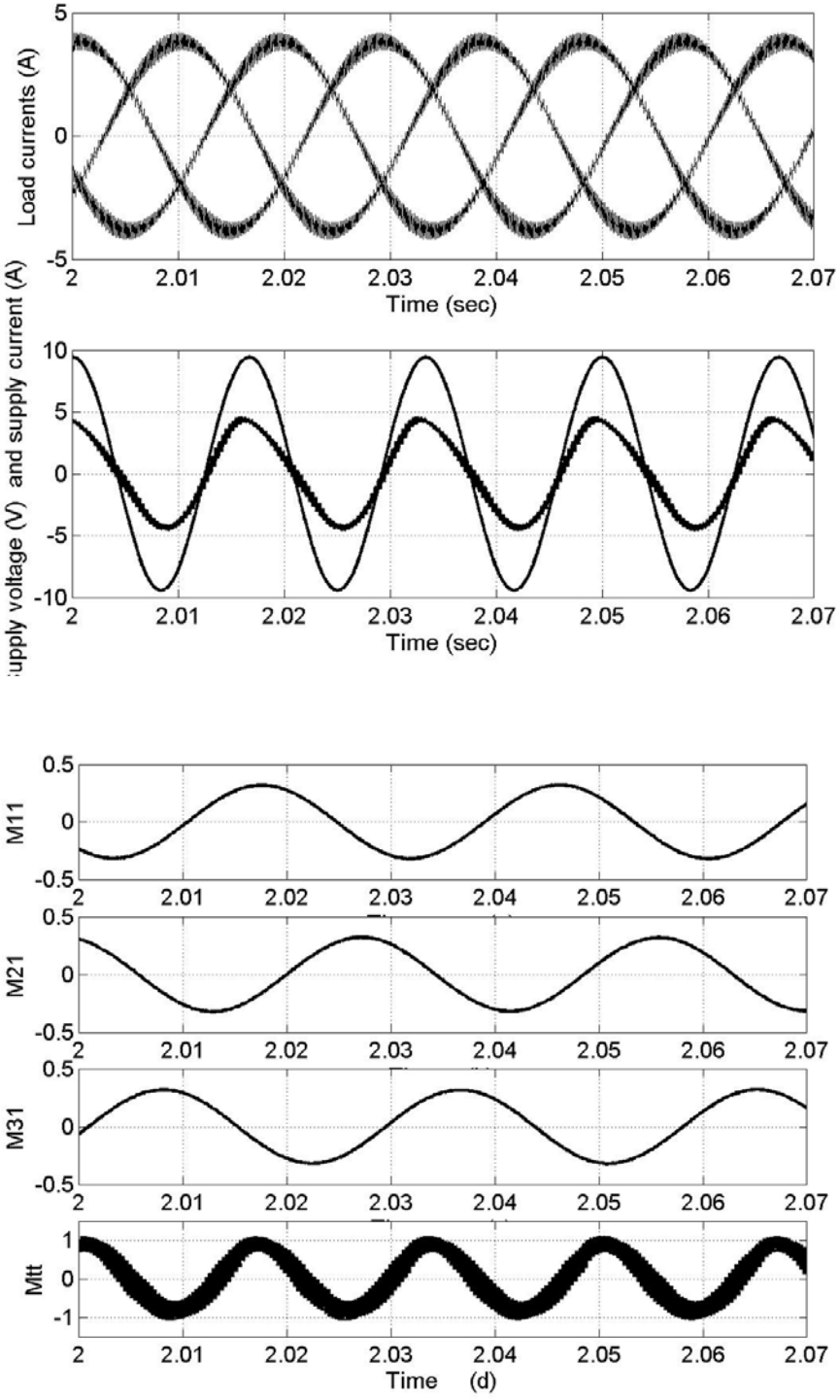

Figure 6.8: On-load of 4 N-m (a) load currents, (b) supply voltage and supply current, (c) the modulation signals M_{11}, M_{21}, M_{31} and Mtt vs time

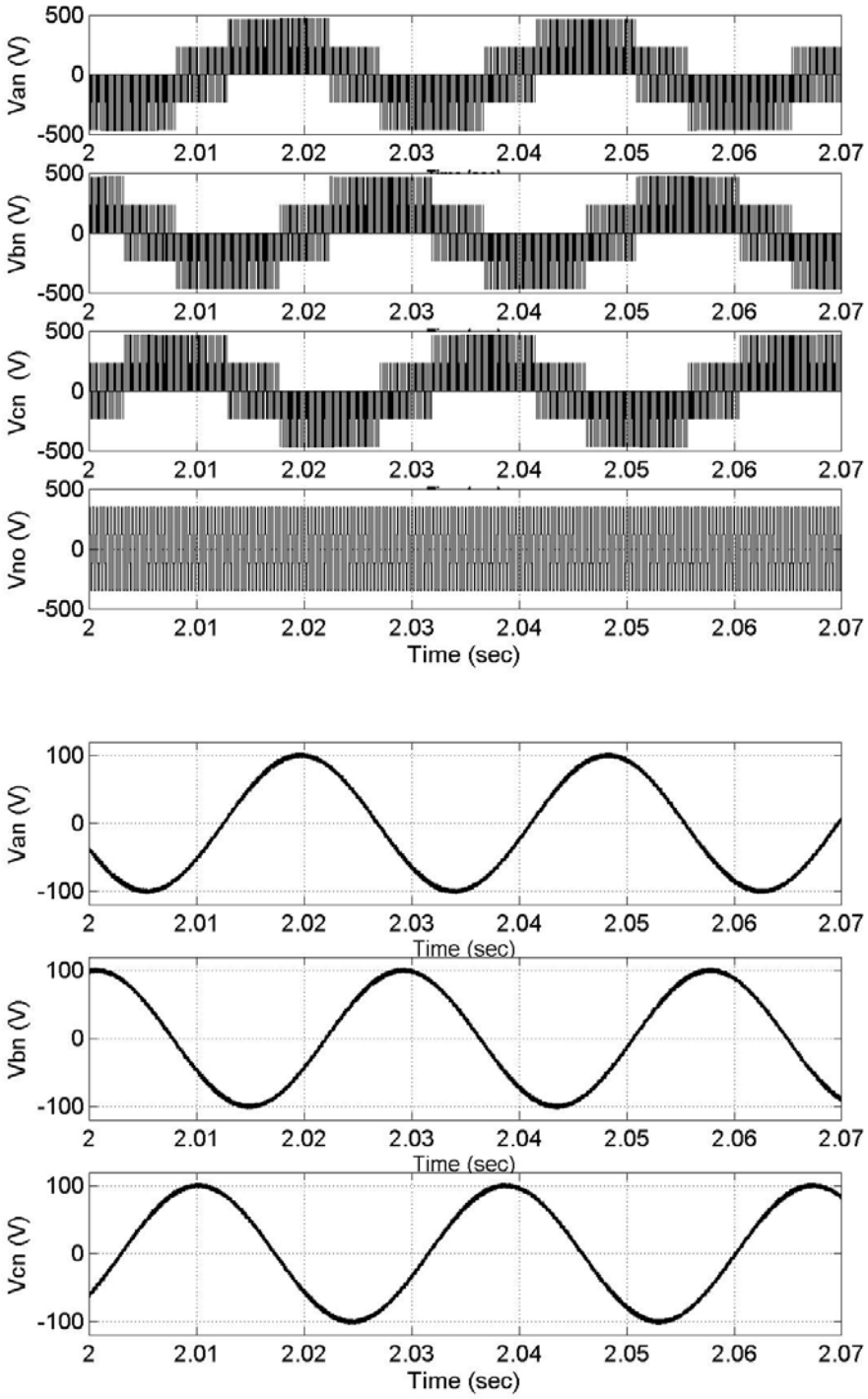

Figure 6.9: On load of 4 N-m (a) The three phase unfiltered load voltages (V_{an} , V_{bn} , V_{cn}) and the zero sequence voltage (V_{no}), (b) The three-phase filtered load voltages V_{an}, (c) V_{bn}, (d) V_{cn}

6.3 Conventional Topology with Reduced Switches

The second topology shown in figure 6.13 is a modification of the circuit analyzed in section 6.2. This inverter reduces the cost by eliminating one of the legs in the load side inverter and so one of the phases is directly connected to the midpoint of the dc link capacitor.

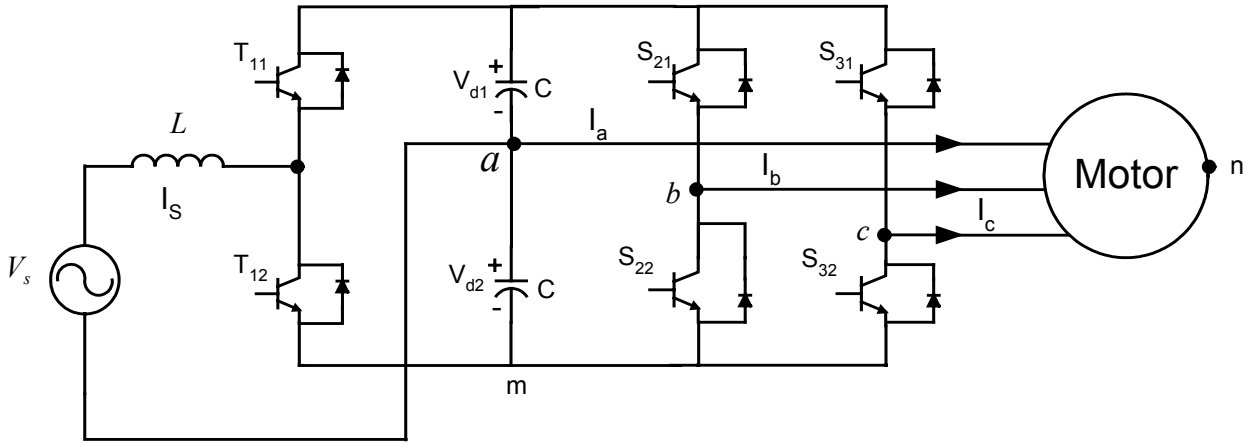

Figure 6.10: Conventional Half-Bridge topology with reduced number of switches.

When compared to the conventional half-bridge converter the above circuit employs less number of switches, thereby reducing the cost of the converter setup, but control wise one of the phase (here 'a') is connected to the dc supply so the control phase 'a' is lost. The equations, which govern the circuit topology, are as follows:

$$V_s - L\frac{di_s}{dt} = V_{d1}T_{11} - V_{d2}T_{12} \tag{6.53}$$

$$V_{d1}S_{21} - V_{d2}S_{22} = V_{bn} + V_{no} \tag{6.54}$$

$$V_{d1}S_{31} - V_{d2}S_{32} = V_{cn} + V_{no} \tag{6.55}$$

where V_{no} is the voltage between the neutral of the load and the midpoint of the dc link voltage and is equal to the negative of the phase voltage V_{an}.

$$V_{an} + V_{no} = 0 \tag{6.56}$$

Adding the Equations 6.54, 6.55 and 6.56 together and knowing that the three phase voltages are to be balanced that is

$$V_{an} + V_{bn} + V_{cn} = 0 \tag{6.57}$$

the expression for V_{no} becomes

$$V_{no} = \frac{1}{3}(V_{d1}(S_{21} + S_{21}) - V_{d2}(2 - S_{21} - S_{31})) \tag{6.58}$$

From the Figure 6.13 it can be observed that the dc link voltage is constant though the voltages V_{d1} and V_{d2} may be different; that is the sum of their voltages is equal to the dc voltage and the difference is the ripple over the dc voltage.

$$V_{d1} + V_{d2} = V_d \tag{6.59}$$

$$V_{d1} - V_{d2} = V_\sigma \tag{6.60}$$

Substituting the switching functions with their modulation signal in Equations 6.35-6.55 the modulation signals become,

$$M_{tt} = \frac{2}{V_d}(V_s - L\frac{di_s}{dt} - \frac{V_\sigma}{2}) \tag{6.61}$$

$$M_{21} = \frac{2}{V_d}(V_{bn} + V_{no} - \frac{V_\sigma}{2}) \tag{6.62 a}$$

$$M_{31} = \frac{2}{V_d}(V_{cn} + V_{no} - \frac{V_\sigma}{2}) \tag{6.63 a}$$

Making use of the condition in Equation 6.56 the Equations in 6.62 (a) and 6.63 (a) can be rewritten as

$$M_{21} = \frac{2}{V_d}(V_{bn} - V_{an} - \frac{V_\sigma}{2}) \tag{6.62 b}$$

$$M_{31} = \frac{2}{V_d}(V_{cn} - V_{an} - \frac{V_\sigma}{2}) \tag{6.63 b}$$

The dc link capacitor current and the ripple are given in Equations 6.64 and 6.65,

$$CpV_d = i_s(2T_{11} - 1) - i_b(2S_{21} - 1) - i_c(2S_{31} - 1) \tag{6.64}$$

The term $(2T_{11} - 1)$ is equal to M_{TT}

$$CpV_\sigma = i_s - i_b - i_c \tag{6.65}$$

In the q and d- axis components the above equations can be written as

$$CpV_d = i_s(2T_{11} - 1) - 1.5\frac{i_{qs}v_{qs}}{V_d} - 1.5\frac{i_{ds}v_{ds}}{V_d} \tag{6.66}$$

The product of the term $i_s(2T_{11} - 1)$ is the product of two time varying signals of the same frequency hence the product gives a fundamental component and a second harmonic component, so equating terms on either side the second harmonic component gets cancelled and so Equation 6.66 can be written as

$$i_s = CpV_d + 1.5\frac{i_{qs}v_{qs}}{V_d} + 1.5\frac{i_{ds}v_{ds}}{V_d} \tag{6.67}$$

The control scheme for this converter is similar to the half-bridge, but due to the lack of control on phase 'a', its voltage is determined by the voltages of phases' b' and 'c' (V_{bn}, V_{cn}). The equations which are useful in designing the controller structure are 6.62, 6.63 6.64 and 6.66. The control scheme can be briefly described as follows; the load that is the induction machine is controlled to maintain a constant speed and rotor flux. The speed command and the flux command give the reference for the q-axis and the d-axis stator current respectively from which the q-axis and the d-axis stator voltages are found which are the outputs of the controller, that is the values of v_{qs} and v_{ds} are the reference voltages to be synthesized by the inverter.

The voltages v_{qs} and v_{ds} are converted back into abc frame using the frequency which is calculated by adding the rotor speed and the slip speed. This gives the three phase voltages (V_{an}, V_{bn}, V_{cn}) from which the modulation signals for the top and the bottom switching devices are found. The switching signals are used to calculate the dc link voltage, which is compared with the reference to output the magnitude of the input supply current which adjusts to any changes in the load. For the supply voltage to be in phase with the supply current, the current is multiplied by the phase of the supply voltage, which is compared with the actual supply current, the difference is regulated to give the modulation signal for the line side converter. Thus in implementing the above control, speed and flux control of the induction machine and unity power factor from the supply is achieved. The controller diagram is a shown in Figure 6.14.

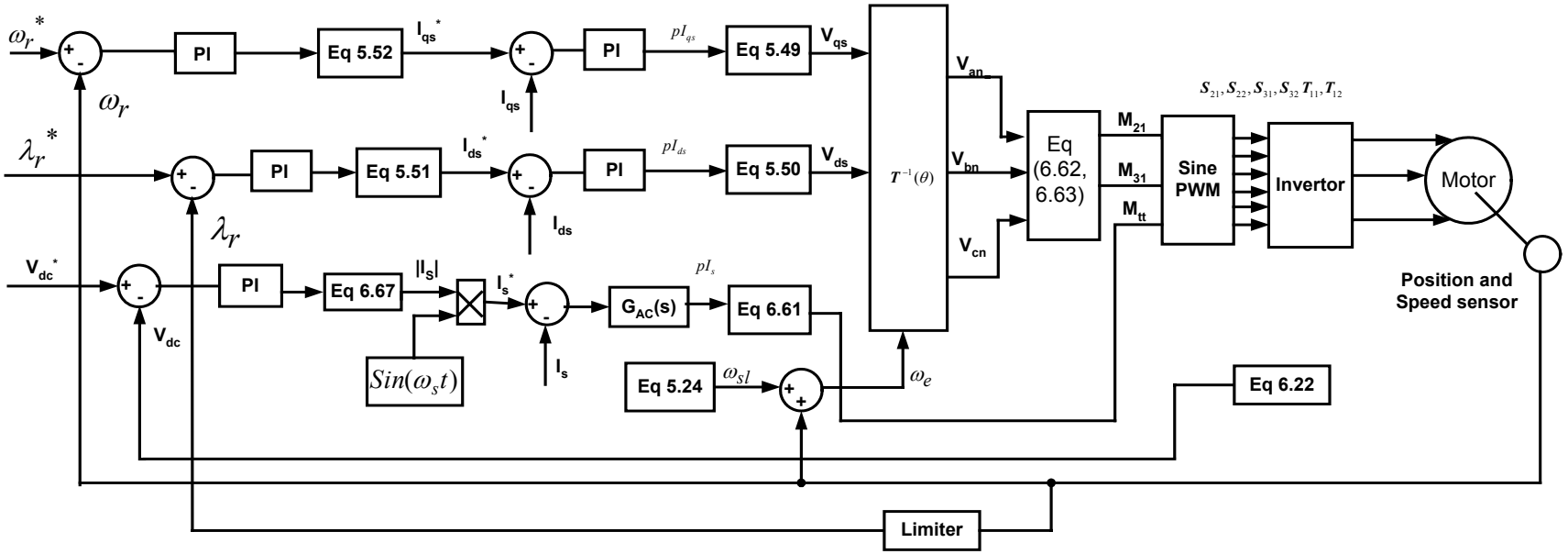

Figure 6.11: Control scheme block diagram for Conventional Half-Bridge topology with reduced switches

6.3.1. Simulation Results

The conventional half–bridge converter with reduced number of switches is simulated for an induction machine. The simulation shows the time response for the various quantities and was done under no-load condition on the motor and after the motor settles to the rated speed, a load of 4 N-m was added at 1s and then the machine was allowed to settle before the load was removed. In Figure 6.12 (a) the regulated dc voltage is shown, it can be seen that the dc voltage drops when the load is added but gradually builds up to almost the reference value and in Figure 6.12 (b) the rotor flux along with its command value is plotted against time.

In Figure 6.13 (a) the load currents when a load of 4 N-m was added is plotted against time and in Figure 6.13 (b) the supply voltage and current are superimposed on each other when the load was added is shown, the supply voltage was scaled down by a factor to clearly show that the current and voltage are nearly in phase with each other.

Figure 6.14 (a) to (d) show the motor frequency, the rotor speed controlled to the reference, the slip speed and the electromagnetic torque when a load of 4 N-m is added are plotted against time. Figure 6.15 shows the unfiltered and the filtered load voltages plotted against the time are shown.

Figure 6.19 shows the modulation signals for the switches in each of the legs, that is for the phase ‘b’, phase ‘c’ and the for the leg connected to the supply voltage (T_{11} and T_{12}).

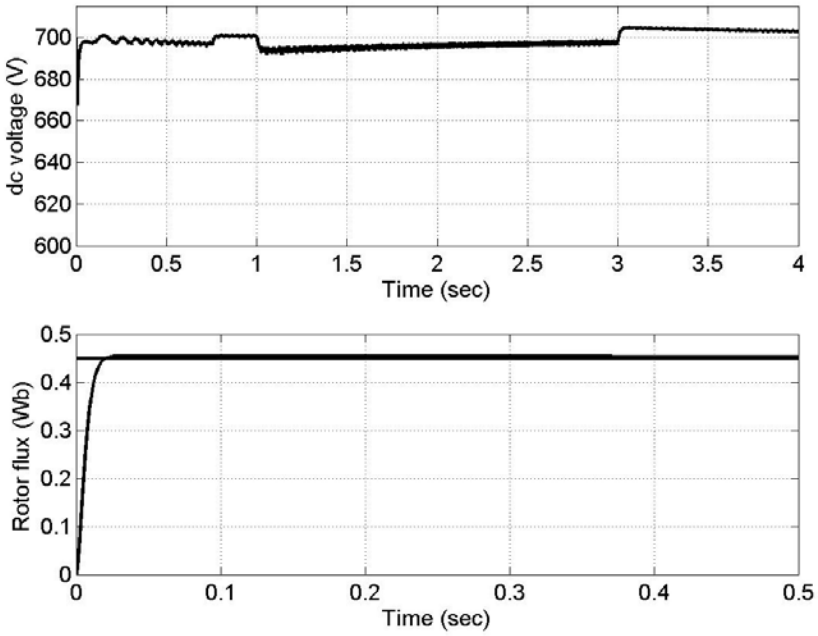

(a)

(b)

Figure 6.12: Regulated dc voltage (a) The dc link voltage for a load change of 4 N-m (b) the rotor flux linkages.

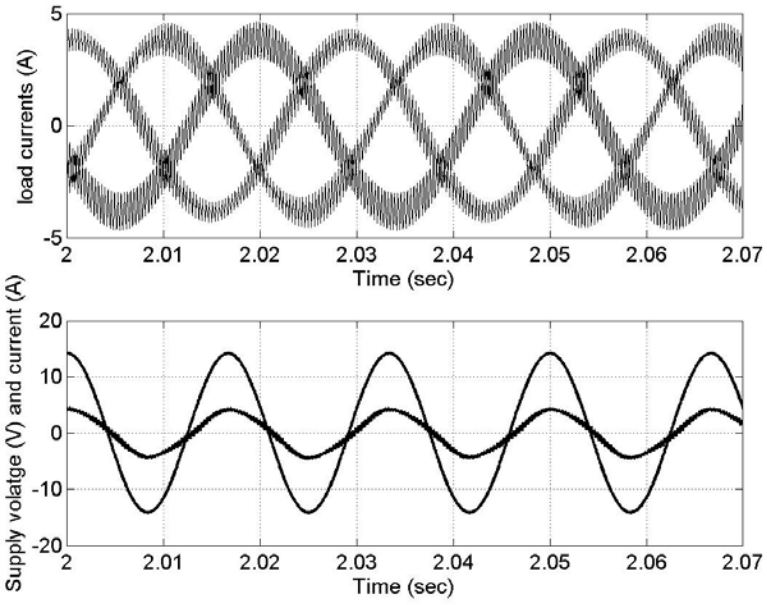

(a)

(b)

Figure 6.13: On-load of 4 N-m (a) load currents, (b) the supply voltage and the supply current.

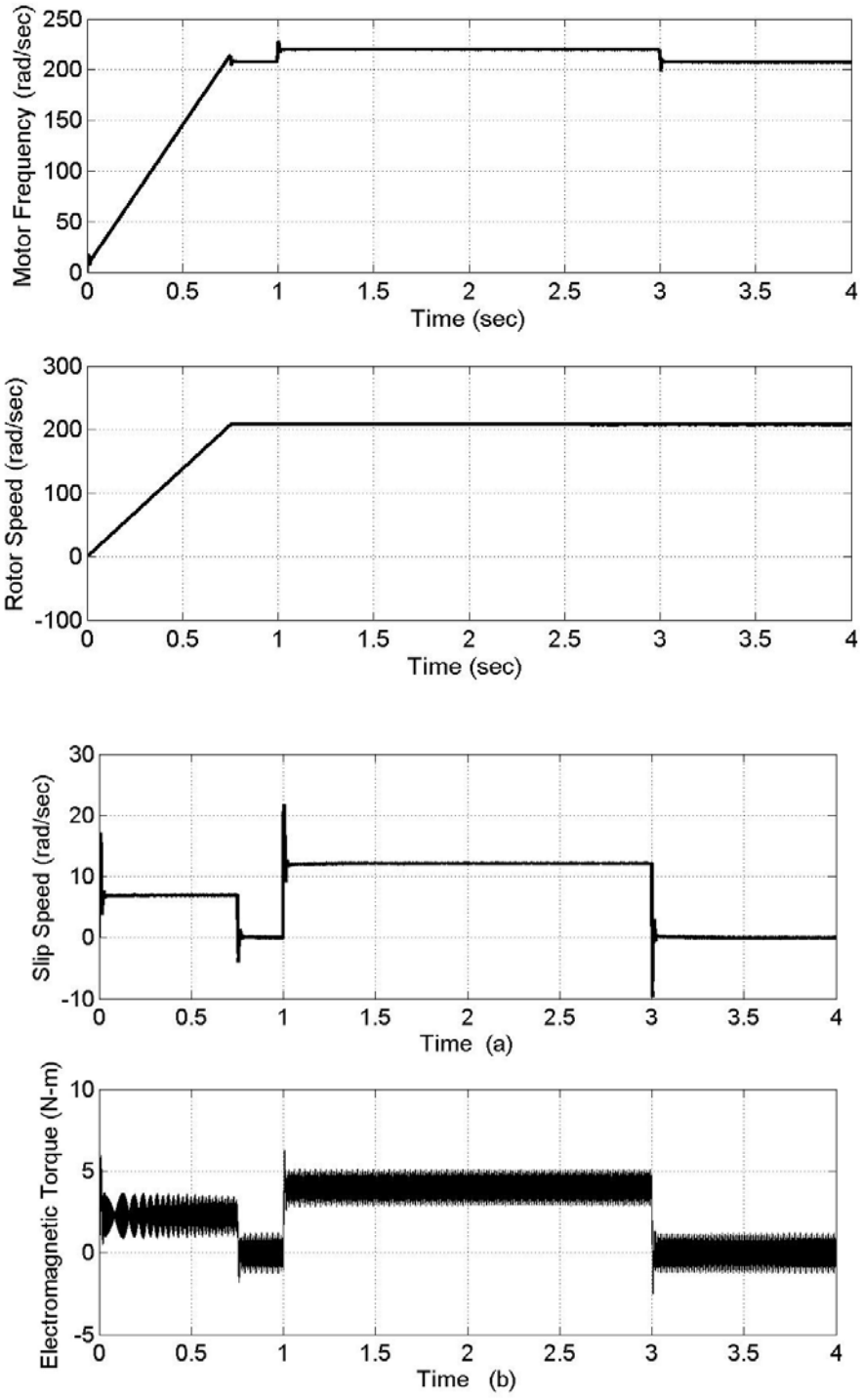

Figure 6.14: Load change (a) the motor frequency in rad/sec, (b) the rotor speed and the command in rad/sec, (c) the slip speed, (d) the electromagnetic torque of 4N-m.

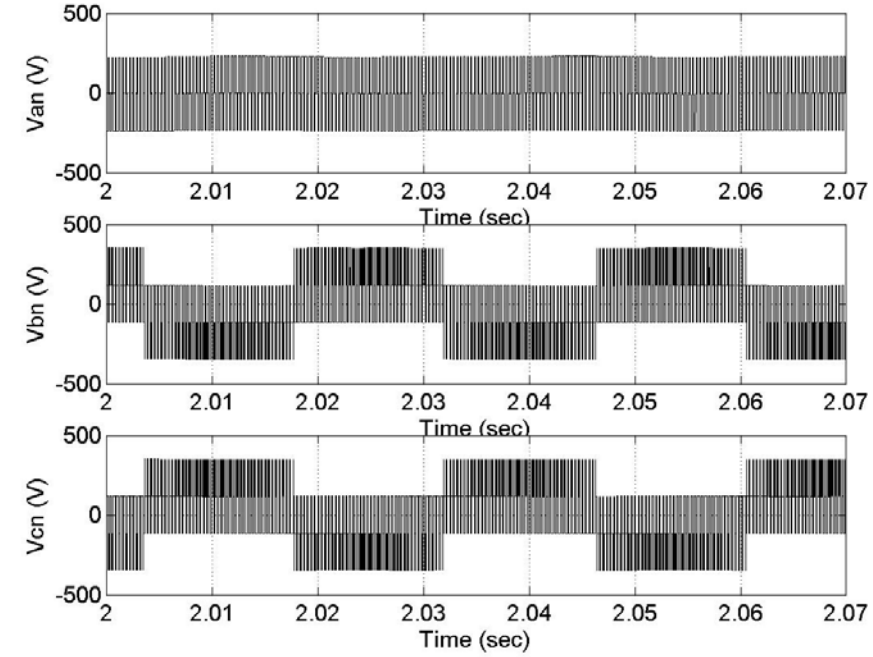

(a)

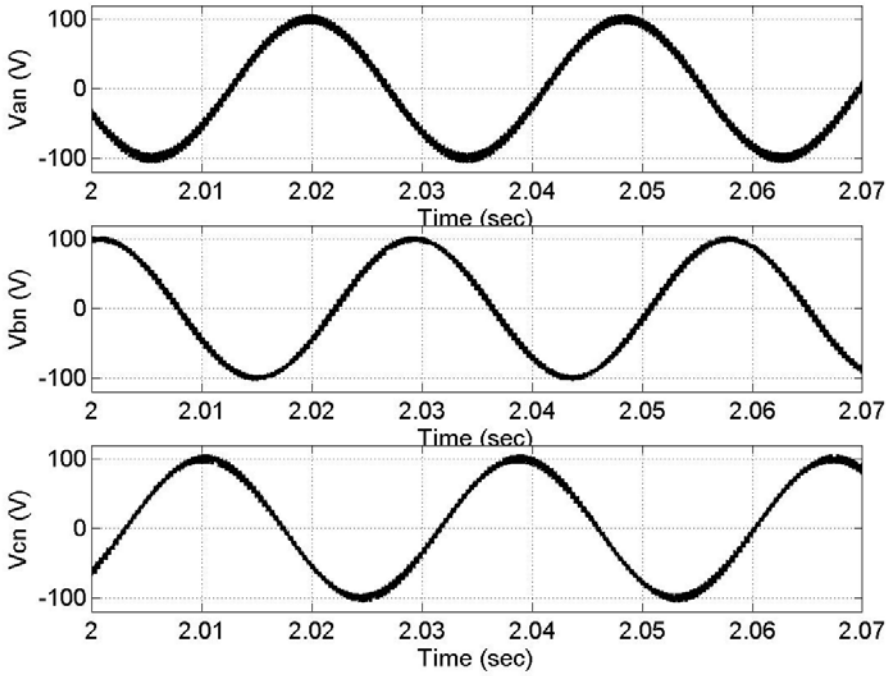

(b)

(c)

(d)

Figure 6.15: On load of 4 N-m (a) the three-phase unfiltered load voltages (V_{an} ,V_{bn} , V_{cn}) , (b) the three-phase filtered load voltages V_{an}, (c) V_{bn}, (d) V_{cn}

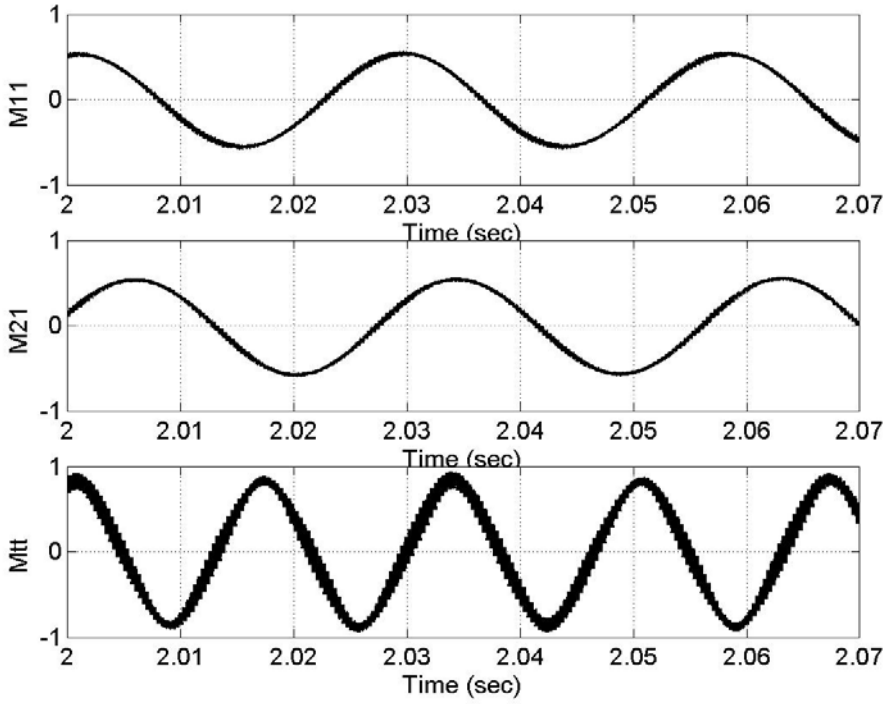

Figure 6.16: On-load of 4 N-m (a) M_{11}, (b) M_{21}, (c) M_{31}

In this chapter two conventional circuits were modeled and a control scheme was set forth for each one of them. Simulation results and detailed analyses of the controlled system confirm the feasibility of these converters to ensure unity input power factor while controlling the motor speed.